Carcinogenesis Advance Access published October 17, 2016

Manuscript Title:

MCM7 and its hosted miR-25, 93 and 106b cluster elicit YAP/TAZ oncogenic activity in lung cancer

Authors:
Lo Sardo F[1], Forcato M[2], Sacconi A[1], Capaci V[5], Zanconato F[3], di Agostino S[1], Del Sal G[5,6], Pandolfi PP[7], Strano S[4], Bicciato S[2], Blandino G[1*].

Running title: YAP/TAZ oncogenic role through microRNA-106b-25.

Affiliations:
[1]Oncogenomic and Epigenetic Unit, Molecular Medicine Area Regina Elena National Cancer Institute, via Elio Chianesi 53, 00144 Rome, Italy.
[2]Center for Genome Research, Department of Life Sciences, University of Modena and Reggio Emilia, via G. Campi 287, 41100 Modena, Italy.
[3]Department of Molecular Medicine, University of Padua School of Medicine, viale Colombo 3, 35126 Padua, Italy.
[4]Molecular Chemoprevention Group, Molecular Medicine Area Regina Elena National Cancer Institute, via Elio Chianesi 53, 00144, Rome, Italy.
[5]Laboratorio Nazionale CIB (LNCIB), Area Science Park Padriciano 99, 34149, Trieste, Italy
[6]Dipartimento di Scienze della Vita-Università degli Studi di Trieste, 34127 Trieste, Italy
[7]Division of Genetics Beth Israel Deaconess Medical Center, CLS Building, Room 401 330 Brookline Avenue Boston, MA 02215

*correspondence should be addressed to G.B (giovanni.blandino@ifo.gov.it).

Abstract

Lung cancer is the first cause of cancer death worldwide and the Hippo pathway transcriptional coactivators YAP/TAZ have a pro-oncogenic role in this context. In order to understand the mechanisms through which YAP/TAZ elicit their oncogenic role in different systems, many studies are focused on YAP/TAZ target genes involved in the regulation of cell proliferation/survival and migration. However, there is scarce evidence on the role of YAP/TAZ in microRNA regulation while there is increasing evidence supporting the role of microRNAs in the main oncogenic processes. Here, we showed that YAP/TAZ were able to regulate several microRNAs in non-small cell lung cancer (NSCLC) cell lines. In detail, we focused on a cluster of three oncogenic microRNAs (miR-25, 93 and 106b) hosted in the MCM7 gene that were overexpressed in lung tumors compared to normal tissues. In addition, similar behaviour was observed in breast cancer and head and neck tumor casuistries, where they showed a prognostic role. In NSCLC cells, YAP/TAZ induced the transcription of the MCM7 gene and its hosted miRs, thereby promoting cell proliferation through the post-transcriptional inhibition of the p21 cell cycle regulator. Accordingly, p21 was maintained at low levels in lung tumors compared to normal tissues. Conversely, its expression was restored in NSCLC cells upon YAP/TAZ interference or upon treatment with the statin cerivastatin. In summary, we provide evidence for a novel mechanism of modulation supporting the protumorigenic functions of the YAP/TAZ factors through the modulation of a bi-oncogenic locus consisting of one gene and three hosted microRNAs.

Keywords: YAP/TAZ, miR-25, 93, 106b, *MCM7*, p21, cell cycle, NSCLC.

Summary: We showed that YAP/TAZ contribute to Non Small Cell Lung Cancer cells proliferation by regulating the expression of MCM7 gene and its hosted microRNAs (miR-25, 93, 106b). These latters contribute to lower p21 expression in tumour compared to normal tissue.

Introduction

Among solid tumors, lung cancer is the first cause of cancer death worldwide and approximately 16.8% of people in the USA diagnosed with lung cancer survive five years after the diagnosis [1]. One of the reasons for this short survival is the fact that most diagnoses are given when the cancer has already progressed beyond a localized state [2]. Approximately 80–85 % of lung cancers are non–small cell lung cancer (NSCLC) [3]. YAP, the final target of the hippo signalling transduction pathway that controls organ size, development, tissue regeneration-homeostasis and stem cell self-renewal (reviewed in [4]) has been shown to work as an oncogene in many solid cancers and it is upregulated or hyperactivated compared to normal tissue (reviewed in [5]). Moreover, higher YAP level or activity correlates with poorer prognosis and shorter patients survival. In that context, YAP transcriptionally activates genes involved in cell proliferation and migration (reviewed in[5]). Accordingly, in lung YAP overexpression has been associated with progression and poor prognosis of NSCLC [6] [7]. Similarly, TAZ, the homologous counterpart of YAP, has been shown as an oncogene in NSCLC [8]. Conversely, AMOT, a scaffold protein that sequesters YAP and TAZ into the cytoplasm inhibiting their nuclear function, decreases lung cancer progression [9]. Moreover, LATS2, a kinase that inhibits YAP/TAZ nuclear function, is frequenty mutated in NSCLC [10]. *In vivo* mouse models showed that overexpression of constitutively active YAP was sufficient to drive lung tumor progression, while knockdown of YAP1 or TAZ decreased *in vitro* cellular migration and transplantation of metastatic disease [11]. Lists of YAP pro-oncogenic target genes have been published from studies on several different experimental mammalian systems and conditions [12] [13] [14] [15] [11] [16, 17], but not in the context of human lung cancer. It is important to note that YAP binding profile genome-wide is very different in tumor cell lines compared to non-tranformed cells[18].

Interestingly, two studies have been published on YAP regulated microRNAs in MCF10A cells [19] or in human pulmonary arterial adventitial fibroblasts (PAAFs) [20] but there is scarce evidence in cancer cell lines or in the tumor context. Alterations in miRNA expression can contribute to tumour growth by inappropriately modulating critical genes involved in tumour cell proliferation, survival and migration. To elucidate the oncogenic role of YAP in the regulation of oncogenic microRNAs we searched for microRNAs upregulated by YAP in lung cancer. We unravelled a YAP/TAZ dependent modulation of a bi-oncogenic locus consisting of one oncogenic gene and three intragenic microRNAs which strongly impinges on the main protumorigenic features of NSCLC cells.

Materials and Methods

Cell culture, transfection and chemical treatment

Human H1299 and H1975 cells were purchased from the American Type Culture Collection (ATCC, Manassas, VA) and routinely tested by PCR for mycoplasma contamination by using the following primers: Myco_fw1: 5'-ACACCATGGGAGCTGGTAAT-3', Myco_rev1: 5'-CTTCATCGACTTTCAGACCCAAGGCA-3'. Cells were grown in RPMI medium (Invitrogen, Carlsbad, CA, USA) supplemented with 10% FBS at 37 °C in a balanced air humidified incubator with 5% CO2. Cells were transfected with Lipofectamine RNAimax (Invitrogen) in accordance with the manufacturer's instruction. siRNAs were used at the final amount of 300 pmols in 60 mm dish. LNA inhibitors for miR-25, 93 and 106b (Exiqon, Vedbæk,Denmark) were used at a final amount of 150 pmols in 60 mm dish. Cerivastatin was purchased from Sigma Aldrich. Cells were treated with dimethylsulphoxide (NT) as a negative control or 1 μM cerivastatin (CER) alone or with 0.5 mM MVA. Cells were collected 48h after transfection or treatment with cerivastatin.

Stable transfection

H1299 cells were transfected using *Lipofectamine® 2000* according to manufacturer instruction with a PIG/22 construct containing a 800 bp intronic sequence that functions as a precursor (pri-miR) of the miR-25, 93 and 106b cluster (PIG-MIR), or with the empty vector as a control (PIG-EV) [21]. 24h after transfection, cells were diluted at 20-30% confluency and fresh medium with 3 μg/μl puromicine was added for selection of stably transfected cells every 3-4 days. Cells were selected for 10-15 days and then they were grown in fresh medium containing 1 μg/μl puromicine, tested for correct miRs overexpression and expanded. For all experiments, cells were mantained in fresh medium containing 1 μg/μl puromicine.

Clonogenic assay

Cells were transfected as indicated above and 24-48 hours later they were detached and seeded at 500 to 1000 cells/well into 6-well dishes (COSTAR). Fresh medium was added every 4 days. Colonies were stained with crystal violet and counted after 7 to 14 days.

FACS cell cycle analysis

For cell cycle analysis, cells were collected 48h after interference or LNA treatment and fixed in 70% ethanol overnight. Fixed cells were treated with RNase at 1 mg/ml final concentration for 30 min at 37°C or overnight at 4°C before adding 5 mg/ml PI and analyzed with Guava Easycyte 8HT flow cytometer equipped with Guava Soft 2.1 (Millipore).

Protein extracts and Western blot analysis

Cells were lysed in buffer with 50mM Tris-Cl pH 7.6, 0,15M NaCl, 5mM EDTA, 1%TritonX-100 and fresh protease inhibitors. Extracts were sonicated for 10+15s and centrifuged at 12000 ×rpm for 10 min to remove cell debris. Protein concentrations were determined by colorimetric assay (Bio-Rad). Western blotting was performed using the following primary antibodies: rabbit polyclonal anti YAP (Santa Cruz, sc-15407), rabbit polyclonal anti TAZ (Sigma anti-WWTR1, HPA007415), mouse monoclonal anti B-actin (ACTBD11B7, Santa Cruz, sc-81178), rabbit monoclonal anti MCM7 (D10A11, Cell Signaling, 3735S), mouse monoclonal anti TEF-1 (BD-Transduction Laboratories, 610923), rabbit monoclonal anti p21 Waf1/Cip1 (Cell Signaling, 2947S), rabbit polyclonal anti Phospho-YAP Ser127 (Cell Signaling, 4911), mouse monoclonal anti HSP90 (Santa Cruz, sc-13119), rabbit polyclonal anti p21 (Santa Cruz, sc-397).

Secondary antibodies used were goat anti-mouse and goat anti-rabbit, conjugated to horseradish peroxidase (Amersham Biosciences,Piscataway, NJ, USA).

MiRNA microarray analysis

The analyses were performed by hybridization on Agilent microarrays of RNA preparations from three independent biological replicates. Briefly, RNA was extracted with TRIZOL and purified using the miRNAeasy® kit (Qiagen, Chatsworth, CA) following the manufacturer's instructions. The concentration and purity of total RNA were assessed using a Nanodrop TM 1000 spectrophotometer (Nanodrop Technologies, Wilmington, DE, USA). Total RNA (100 ng) was labeled with miRNA Hybridization kit (Agilent Technologies) according to manufacturer instructions and hybridized to Human miRNA Microarray V19 (Agilent Technologies). Scanning and image analysis were performed using the Agilent DNA Microarray Scanner (P/N G2565BA) equipped with extended dynamic range (XDR) software according to the Agilent miRNA Microarray System with miRNA Complete Labeling and Hyb Kit Protocol manual. Feature Extraction Software (Version 10.5) was used for data extraction from raw microarray image files using the miRNA_107_Sep09_1_1_QC protocol. A Z-score transformation was performed to express the background corrected spot intensity values as a unit of standard deviation from the normalized mean of zero. Features were selected based on Z-ratios calculated as the difference between the averages of the observed miRNA's Z-scores divided by the standard deviation of all the differences of the comparison. Absolute Z-ratios higher than 1.5 were inferred as significant. Deregulated miRNAs were used for hierarchical clustering (see also Supplementary tables S1a ans S1b).

MiRNA and transcript analysis

Total RNA was extracted using TRIzol (Ambion) according to the manufacturer's recommendations. For miR analysis, 30 ng RNA were retrotranscribed using the TaqMan microRNA Reverse Transcription Kit (Applied Biosystem) and Real time-PCR of miR expression was carried out in a final volume of 10 ul using TaqMan MicroRNA® Assays (Applied Biosystems) and normalized on RNU48 and RNU49 as endogenous controls. We

have chosen RNU48 and RNU49 because they were not modulated in our experimental conditions. Conversely, we found that other RNU (RNU19, RNU44 or RNU6b) were modulated and we could not use them for our purposes. TaqMan probes for miRNAs and RNU were purchased from Applied Byosistem. For gene transcript analysis, 1γ RNA was retrotranscribed using M-MLV reverse transcriptase (Invitrogen) following the manufacturer instructions. Real time PCR was performed in a final volume of 10 ul using KAPA Sybr Fast ABI Prism qPCR master mix (Kapa Biosystems, Woburn, MA, USA), and normalized on GAPDH. All the real time PCR analyses were performed on a StepOne instrument (Applied Biosystems).

ChIp analysis

ChIP-qPCR was performed as described previously in ref. [16]. Briefly, cells were fixed with1% formaldehyde (Sigma) in culture medium for 10min at room temperature, and chromatin from lysed nuclei was sheared to 200–600bp fragments using a Bioruptor sonicator (Diagenode). 100µg of sheared chromatin and 5µg of antibody plus 40µl of magnetic beads (Dynabeads® Protein G 10004D ThermoFisher) were used for each Ip. Rabbit monoclonal anti YAP (Abcam, ab52771) and rabbit anti IgG (H-270, Santa Cruz sc-66931) were used. Quantitative real-time PCR was carried out with a StepOne instrument (Applied Biosystems). Each sample was analysed in triplicate. The amount of immunoprecipitated DNA in each sample was determined as the fraction of the input (amplification efficiencyˆ(Ct INPUT–Ct ChIP)), and normalized to the IgG control.

Luciferase assay

For Luciferase assay H1299 or H1975 cells were co-transfected in 24-well dishes using Lipofectamine 3000 (Invitrogen) with 100ng of pGL3-Basic containing a p21$^{Waf1/Cip1}$ 3'UTR-firefly luciferase reporter (a kind gift of Dr. Arnold Gruenweller, Philipps-Marburg University, 35032 Marburg, Germany), *the same vector with a 3bp deletion in the seed sequence recognized by miR-25, 93 and 106b* or pGL3 empty vector as a control, plus 10

ng of the transfection control Renilla vector (pRLTK, Promega), and the LNA Negative Control or LNA inhibitor for miR-25, 93 and 106b at a final amount of 25 pmol/well. Cells were harvested 24-48 hours post transfection and luciferase activities were analyzed by the dual-luciferase reporter assay system (Promega, Madison, WI) in the GloMax 96 Microplate Luminometer (Promega). *Mutagenesis was performed through* QuikChange II Site-Directed Mutagenesis Kit *(Agilent technologies) following the manufacturer's instructions and using the nucleotides listed below*: del61-63-antisense: 5'-cttcatttgtctaccgaacttccccggagtgg-3'; del61-63-sense: 5'-gaagtaaacagatggcttgaaggggcctcacc-3'. Correct deletion was confirmed by plasmid Generation of

Sequence of siRNA used for interference

siGFP (as nonsilencing control) 5'-AAGUUCAGCGUGUCCGGGGAG-3', siYAP#1: 5'-GACAUCUUCUGGUCAGAGA-3', siYAP#2: 5'-CUGGUCAGAGAUACUUCUU-3', siTAZ#1: 5'-AAAGUUCCUAAGUCAACGU-3', siTAZ#2: 5'-AGGUACUUCCUCAAUCACA-3', siMCM7#1: 5'-UACUACGAGGGAUAUUUCCUU-3', siMCM7#2: 5'-GAUCACACGAGGCUUGUUGUU-3', siLATS1: 5'- CAUACGAGUCAAUCAGUAA-3', siLATS2: 5'-GCCACGACUUAUUCUGGAA-3', siTEAD1#1: 5'-CGAUUUGUAUACCGAAUAA-3', siTEAD1#2: 5'-GAAAGGUGGCUUAAAGGAA-3'.

Sequence of primers used for transcript analyses

RT-MCM7-F: 5'-TCGAGGCATGAAAATCCGGG-3', RT-MCM7-R: 5'-CGCCAGTCGATCAATGTATGACA-3', RT-YAP-F:5'-CACAGCATGTTCGAGCTCAT-3', RT-YAP-R: 5'-GATGCTGAGCTGTGGGTGTA-3', RT-TAZ-F: 5'-CCATCACTAATAATAGCTCAGATC-3', RT-TAZ-R: 5'-GTGATTACAGCCAGGTTAGAAAG-3', RT-TEAD1-F: 5'-CCACCAAAGTTTGCTCCTTTGGGA-3', RT-TEAD1-R: 5'-ACTTCAAACACACAGGCCATGCAG-3', RT-LATS1-F: 5'-CTCTGCACTGGCTTCAGATG-

3'; RT-LATS1-R, 5'-TCCGCTCTAATGGCTTCAGT-3', RT-LATS2-F: 5'-ACATTCACTGGTGGGGACTC-3', RT-LATS2-R: 5'-GTGGGAGTAGGTGCCAAAAA-3'; RT-GAPDH-F 5'-GAGTCAACGGATTTGGTCGT-3', RT-GAPDH-R: 5'-GACAAGCTTCCCGTTCTCAG-3', RT-premiR25-F: 5'-GTGTTGAGAGGGCGGAGACTT-3'; RT-premir25-R: 5'-TCAGACCGAGACAAGTGCAA-3', RT-premiR93-F: 5'-AAGTGCTGTTCGTGCAGG-3', RT-premiR93-R: 5'-CTCGGGAAGTGCTAGCTCA-3', RT-premiR106b-F: 5'-GCTGACAGTGCAGATAGTGGTCCT-3', RT-premiR106b-R: 5'-TGGAGCAGCAAGTACCCACAGT-3', RT-CTGF-F: 5'-GCCACAAGCTGTCCAGTCTAATCG-3', RT-CTGF-R: 5'-TGCATTCTCCAGCCATCAAGAGAC-3', RT-ANKRD1-F: 5'-AGTAGAGGAACTGGTCACTGG-3', RT-ANKRD1-R:5'-TGGGCTAGAAGTGTCTTCAGAT-3', RT-p21-F: 5'-GGGACAGCAGAGGAAGAC-3', RT-p21-R: 5'-GCGTTTGGAGTGGTAGAAATC-3'.

Sequence of primers used for ChIp

ChIP-CTGF-F: 5'- CTTTGGAGAGTTTCAAGAGCC-3'; ChIP-CTGF-R: 5'-TCTGTCCACTGACATACATCC-3'; ChIP-MCM7enh-F: 5'-CAGAACTCGGATTAGGGCTG-3'; ChIP-MCM7enh-R: 5'-GCT TGGGAAGTGAGTCAAAACT-3'; ChIP-H1H2BA-F: 5'- ACTCTCCTTACGGGTCCTCTTG-3'; ChIP-H1H2BA-R- AGTGCTGTGTAACCCTGGAAAA.

Differentially expressed miRNAs or genes

Deregulation of miRNAs or genes in different set of patient samples was assessed by two tailed student's T-test, and a false discovery rate procedure (Storey, 2002) was performed to take into account multiple comparisons. Significance level was set to 5%. Analyses were performed by Matlab (The MathWorks Inc.).

Curves of Recurrence Free Survival (RFS)

Curves of Recurrence Free Survival in HN patients were evaluated by Kaplan-Meier method. The expression levels of the samples were sorted to obtain three subgroups with high, medium or low signal for each miRNA. Curves of patients with high and low signals were considered to establish statistical significance by using the logrank test. Calculation of the miRNA score signature was obtained as described in [22]. Analyses were performed by Matlab (The MathWorks Inc.).

Results

MCM7 and hosted miR-25, 93 and 106b are regulated by YAP in Non Small Cell Lung Cancer

In order to find potential microRNAs regulated by YAP in the NSCLC context, we knocked down the expression of YAP in the H1299 non-small cell lung cancer cell line (Supplementary Figure S1a, left panel). MicroRNA profiling of the siYAP transfected cells (as compared to their control counterparts) revealed that several microRNAs were downregulated (Supplementary Figure S1a, right panel). Thus, we hypothesized that those microRNAs would be bona fide YAP driven oncogenic microRNAs (Supplementary table S1a and b). Among them, miR-130b-3p, miR-29a-3p, miR-29b-3p and miR-29c-3p result regulated by YAP in agreement with recent reports[19, 20] (Supplementary Figure S1b). We focused our attention on miR-25-3p, miR-93-5p and miR-106b-5p that belong to an intragenic cluster (named microRNA-106b-25 cluster) located in intron 13 of *MCM7* (Minichromosome Manteinance complex 7) gene (Figure 1a) [21]. These are oncogenic microRNAs that induce both cell proliferation and migration and are overexpressed in several tumors together with the *MCM7* host gene [23] [24, 25] [26]. Moreover, MCM7 has been shown to be an important prognostic marker in lung cancer [27] [28] [29]. *MCM7* is a member of a family of DNA helicases important for initiatig DNA replication and for cell cycle progression [30]. In H1299 cells depleted of YAP protein, we confirmed that miR-25, 93 and 106b expression decreased and further observed a reduction in the MCM7 mRNA level (Figure 1b). This result is paired with two previous studies where *MCM7* was shown to be upregulated upon YAP or TAZ overexpression in MCF10A cells[13, 31] and with a recent work where *MCM7* has been shown to be a YAP/TAZ transcriptional target in breast cancer cell lines by ChIP-seq (see below) [16].

Downregulation of YAP/TAZ, MCM7 and miR-25, 93 and 106b affects cell proliferation in NSCLC

YAP was shown to work redundantly with TAZ in several model systems[16, 32]. In agreement with this, we observed that simultaneous knockdown of YAP and TAZ synergistically affected colony forming ability in H1299 cells (Figure 1c, Supplementary Figure S1d), as compared to the single treatments. This also induced an increased cell number in the G1 phase and a reduction in the number of cells in the S and G2 phase (Supplementary Figure S1e) suggesting proliferation inhibition. We observed the same effects in another NSCLC cell line, H1975 (Figure 1e, Supplementary Figure S1f, g). Interestingly, either siRNAs-mediated downregulation of MCM7 or LNAs mediated inhibition of miR-25, 93 and 106b strongly phenocopied the effect of YAP/TAZ interference in both cell lines (Figure 1d, f, g, h, Supplementary Figure S1h-m).

YAP, TAZ and TEAD regulate the expression of MCM7 gene and its hosted microRNA cluster

As mentioned above, Zanconato and colleagues showed that YAP and TAZ regulated several cell cycle related genes, among those *MCM7*. In detail by performing ChIP-seq experiments and integrating their data with previously reported high-resolution maps of chromatin interactions (Hi-C) the authors observed the binding of YAP/TAZ to a distal enhancer that interacts with the *MCM7* promoter in a breast cancer cell line [16] (Figure 2a). In the latter context, YAP/TAZ cooperated with the TEAD transcription factors that are often associated with YAP/TAZ in the upregulation of their oncogenic targets[13, 31]. To explain in detail the abovementioned observations and to match them with our findings, we assessed the levels of the miR-25, 93 and 106b precursors (pre-microRNA) in the YAP/TAZ siRNA-transfected H1299 and H1975 cells. We observed that YAP/TAZ interference induced a significative downregulation of MCM7 transcript and hosted miR

precursors with two alternative siRNAs (figure 2b, c, Supplementary Figure S1n, o). Moreover, we observed that the TEAD1 transcription factor was involved in the regulation of the mature miRNAs, their precursors and their host gene *MCM7* (Figure 3a, b, Supplementary Figure S2a, b). In addition, we observed a stronger effect when TEAD1 and YAP were simultaneously depleted. As control, we analysed the mRNA abundance of two well-known YAP/TAZ transcriptional targets, CTGF and ANKRD1 whose levels were expectedly reduced upon YAP/TAZ and TEAD interference in both cell lines (Figure 3c, d, Supplementary Figure S2c-f). Conversely, the knockdown of Lats1 and Lats2, two inhibitors of YAP and TAZ activity, determined an increase in the target gene transcripts (Supplementary Figure S2e, f). We obtained the same results also by using alternative siRNA directed against YAP and TAZ (Supplementary Figure S3a, b).

Interestingly, two recent reports showed that YAP/TAZ activity is controlled by the mevalonate (MVA) metabolic pathway. The geranylgeranyl pyrophosphate, an intermediate of the mevalonate cascade, is required for activation of Rho GTPases that, in turn, inhibits YAP/TAZ phosphorylation thus promoting their nuclear accumulation. Treatment of different cell lines with statins, inhibitors of the upstream steps of this pathway, caused TAZ degradation and YAP/TAZ hyperphosphorylation and translocation from the nucleus to the cytoplasm, thus inhibiting their nuclear function in transcriptional activation of pro-oncogenic genes and reducing tumor growth in mice xenograft [33, 34] [35].

We treated H1299 cells with the statin cerivastatin in order to check whether we could recapitulate the effects observed upon YAP/TAZ interference. Upon cerivastatin treatment, we observed an increased phosphorylation of YAP and decreased TAZ level confirming previous results[33] (Supplementary Figure S3c, left panel). Strikingly, we observed a reduction in MCM7 protein and transcript, while concomitant treatment with MVA reversed

cerivastatin effect (Supplementary Figure S3c, left and right panels). Finally, we performed chromatin immunoprecipitation analysis (ChIP) in both H1299 and H1975 and we observed the binding of YAP onto the enhancer region regulating *MCM7* gene (Figure 3e, f). Together, these results strongly suggest that the *MCM7* locus behaves as a canonical Hippo pathway target.

YAP/TAZ and TEAD lower p21 expression through MCM7 and its hosted microRNAs

In silico analysis of The Cancer Genome Atlas (TCGA) revealed that a high expression of the miR-25, 93, 106b and of the MCM7 mRNA was significantly enriched within lung cancer tissues as opposed to normal tissues (Figure 4a). In addition, coordinated enrichment for the mentioned miRNAs in the tumour tissues was observed in a breast cancer casuistry and in a head and neck tumour casuistry previously studied by our group [36] [22] (Supplementary Figure S4a and S4b, upper panels, Supplementary Table S2). Further, in the analysed head and neck cancer patients, we observed a higher recurrence probability in patients overexpressing miR-25, 93 and 106b (Supplementary Figure S4b, lower panels).

In order to address the oncogenic role of YAP/TAZ exerted through the regulation of miR-106b-25 cluster, we searched for transcripts anti-correlated to miR-25, 93 and 106b in the TCGA lung cancer and that could be bona fide targets of at least one of these miRNAs as calculated by three different prediction softwares (Supplementary table S3, Supplementary table S4, sheet 1). This could provide information about potential targets that might be clinically relevant in lung cancer. Pathway enrichment analysis and functional classification of the obtained transcripts list with DAVID functional annotation revealed that the identified genes belonged mainly to focal adhesion, calcium signaling and cancer pathways (Supplementary table S4, sheets 2 and 3, Figure 4b). We focused on this latter category and in particular on CDKN1A (Cyclin-Dependent Kinase inhibitor 1A) encoding for the p21

protein, also known as p21WAF1/Cip1, a negative regulator of the cell cycle (Supplementary table S4, sheet 2, Supplementary Figure S4c). We chose CDKN1A for several reasons:

1- it has already been shown to be a target of miR-93 and miR-106b [23]. To further validate this in our system, H1299 and H1975 cells co-*transfected with the pGL3 plasmid containing p21-3'UTR cloned downstream* the firefly luciferase gene along with LNA inhibitors for miR-25, 93 and 106b showed a higher firefly luciferase signal *compared to cells co-transfected with the same vector and with control LNA. T*his effect was abrogated when the *p21-3'UTR was mutated in the seed sequence recognized by those microRNAs (Supplementary Figure S5a, b).*

2- Strikingly, p21 was downregulated in tumoral vs normal tissues in the lung TCGA casuistry (Figure 4c) as opposite to MCM7 and hosted miRs (Figure 4a). In H1299 and H1975 cells, p21 protein and transcript were increased upon YAP, TAZ and TEAD siRNA-mediated knockdown as well as upon cerivastatin treatment, while concomitant treatment with MVA rescued normal p21 levels (Figure 5a-d, Supplementary Figure S4d, Supplementary Figure S5c, d). These results strongly suggest that nuclear YAP/TAZ and TEAD are required to maintain p21 at low level in tumors.

3- Two previous reports showed that YAP represses CDKN1A in different experimental systems. However, they highlighted two transcriptional mechanisms. One mechanism involved YAP/RUNX2 cooperation in the direct transcriptional repression of p21 (Figure 5e, left panel) [37]. The second work proposed an indirect mechanism whereby YAP repressed Lats2 that was no longer able to cooperate with p53 in the transcriptional activation of p21 [38] (Figure 5e, right panel). Since the H1299 cells are p53 null, we could exclude the p53 dependent mechanism of CDKN1A regulation in our experimental system. Interestingly interference for MCM7 caused a reduction of miR-25, 93, 106b level

(Supplementary Figure S5e, f) and a concomitant increase of the p21 protein and transcript (Figure 6a-d). LNA treatment efficiently reduced the amount of the three microRNAs (Supplementary Figure S5g, h) and increased p21 protein and transcript level without affecting the MCM7 protein and mRNA (Figure 6e, f). These results suggested that p21 accumulation following YAP/TAZ knockdown could be mediated at least in part by the reduction of MCM7 transcript and hosted miR-25,93 and106b thus linking for the first time YAP and p21 through post-transcriptional mechanisms mediated by microRNAs.

To strengthen this hypothesis we performed a rescue experiment with H1299 cells stably transfected with a construct expressing the 800 base pair intron containing miR-25, 93 and 106b, or with empty vector as a control [21]. Control cells stably transfected with an empty vector (EV) and cells overexpressing miR 106b-25 cluster (MIR) (Supplementary Figure S6a) were knocked-down for YAP/TAZ and for MCM7 and analyzed for p21 expression and cell cycle distribution. Strikingly, p21 protein was increased upon YAP/TAZ and MCM7 interference but this effect was reduced upon concomitant miR-25, 93 and 106b overexpression (Supplementary Figure S6b). Moreover, we observed an accumulation of cells in G1 and a concomitant reduction of cells in S and G2 upon YAP/TAZ and MCM7 interference, and this effect was slightly reduced upon concomitant miRs overexpression (Supplementary Figure S6c). The effect of miR-25, 93 and 106b overexpression in reducing p21 protein accumulation upon YAP/TAZ and MCM7 interference is clear. However, the biological effect of the overexpression of this miR cluster on cell cycle distribution is rather mild. This might also be due because YAP/TAZ and MCM7 affect several different pathways that converge to modulate important cell cycle regulators like p21 protein, while miR-25, 93 and 106b cluster is only a piece of the puzzle contributing to this effect together with other several players.

Discussion

In this work, we provide an example of how YAP and TAZ can elicit their oncogenic function by employing both transcriptional and post-transcriptional mechanisms, through the simultaneous upregulation of the oncogenic *MCM7* gene and its three hosted miR-25, 93 and 106b (Figure 6g). Our findings extend current knowledge on the role of YAP/TAZ in microRNA abundance regulation in addition to the previously characterized role of YAP/TAZ in post-transcriptional microRNA processing through the modulation of Dicer and p72 microprocessor activity [39, 40]. Interestingly, the MCM7 gene locus in mice has been defined as a bi-oncogenic locus because both MCM7 protein and hosted miRNAs together (and not singularly) were required for cellular transformation and for initiating prostate tumorigenesis. In the latter work, miR-25, 93 and 106b were shown to exert their oncogenic role in part by regulating PTEN abundance [21]. In our study, these miRNAs do not strongly affect PTEN level, probably because other feedback mechanisms may prevent the alteration of its abundance (data not shown). However, these miRNAs regulate other important genes involved in oncogenic processes, one of which is p21 (Figure 6e, f). Moreover, it is likely that the reduction of MCM7 protein level independently of hosted miRs can have an impact on p21 abundance and cell cycle progression from G1 to S phase, because it has been already shown that alterations in MCM7 protein level (both for excess or deprivation) can activate cell cycle checkpoint [41, 42]. Downregulation of p21 abundance by YAP/TAZ through an indirect mechanism mediated by both MCM7 gene and hosted microRNAs may happen concomitantly with the other proposed transcriptional mechanisms (Figure 5e, mid panel). This is an example of how several distinct mechanisms orchestrated by YAP/TAZ converge to modulate important cell cycle regulators whose abundance needs to be finely tuned in the cell and whose dysregulation provides the targeted cells with protumorigenic properties.

It is likely that other YAP/TAZ targets may act as coding-independent players in regulating oncogenic processes in addition to microRNAs. For example, competing endogenous RNA (ceRNA), long non coding RNA (lncRNA), enhancer associated RNA (eRNA) are emerging for their role in development and cancer beyond the direct transcriptional regulation of genes[43] [44] [45, 46]. In favour of this hypothesis, recently YAP and TAZ have been mapped at enhancers much more frequently than in proximity of transcription start sites [16]. It will be interesting in the future to deeply characterize these potential targets. Importantly, treatment of NSCLC cells with statin phenocopies what observed upon YAP/TAZ interference. This reinforces previous experimental evidences in mouse tumor models and epidemiological data in humans showing tumour suppressing effects of statins [47] [48] and further strengthens the concept that statins may be promising therapeutic inhibitors of YAP/TAZ oncogenic activity [33] [34].

A deeper understanding and analysis of the multiple layers regulating oncogenic mechanisms could be relevant for the characterization of novel prognostic factors in cancer and for the development of novel anti-cancer therapies.

LEGENDS TO FIGURES

Figure 1. YAP regulates microRNA-106b-25 cluster and host gene *MCM7*. Downregulation of YAP/TAZ, MCM7 and hosted microRNAs affects proliferation of NSCLC. (**a**) Schematic representation of *MCM7* locus containing miR-25, 93 and 106b in its 13th intron. (**b**) Taq-Man based quantification of mi-R25, 93 and 106b normalized to RNU48 and real-time based quantification of MCM7 and YAP transcripts normalized to GAPDH in YAP interfered cells (siYAP#1) respect to control (siGFP) H1299 cells. Data points were generated from the average of at least three independent biological replicates. SEM is indicated. Asteriscs represent statistically relevant results calculated using Two-tailed t test. P and n values: miR-25 siYAP#1/siGFP p=0,003 n=6, miR-93 siYAP#1/siGFP p=0,04 n=3, miR-106b siYAP#1/siGFP p=0,02 n=3, MCM7 siYAP#1/siGFP p=0,006 n=4, YAP siYAP#1/siGFP p=0,001 n=3. (**c-f**) Clonogenic assay of H1299 (**c, d**) and H1975 cells (**e, f**) upon YAP, TAZ, YAP/TAZ and MCM7 interference with two alternative siRNAs compared to siGFP control cells. (**g,h**) Clonogenic assay of H1299 (**g**) and H1975 cells (**h**) treated with LNA inhibitors for miR-25, 93 and 106b at a final amount of 150 pmols in 60 mm dish. Data are presented as mean +-SEM. Two-tailed t test analysis was applied to calculate the p values. H1299 siYAP#2/siGFP p=0,05 n=3, siTAZ#1/siGFP p=0,02 n=3, si TAZ#2/siGFP p=0,01 n=3, siYAP#1TAZ#1/siGFP p=0,0001 n=3, siYAP#2TAZ#2/siGFP p=0,0007 n=3, siMCM7#1/siGFP p=6,69x10^-5 n=3, siMCM7#2/siGFP p=0,0002 n=3. H1975 siYAP#1/siGFP p=0,03 n=3, siYAP#2/siGFP p=0,006 n=3, siTAZ#1/siGFP p=0,005 n=3, siTAZ#2/siGFP p=0,006 n=3, siYAP#1TAZ#1/siGFP p=2,8X10^-13 n=3, siYAP#2TAZ#2/siGFP p=1,2x10^-5 n=3, siMCM7#1/siGFP p=0,0002 n=3, siMCM7#2/siGFP p=9,8X10^-6 n=3. H1299 LNAmiR-25/ctrl p=0,002 n=3, LNAmiR-25,93,106b/ctrl p=0,003 n=3, H1975 LNAmiR-25/ctrl p=0,006 n=3, LNAmiR-93/ctrl p=0,02 n=3, LNAmiR-106b/ctrl p=0,05 n=3, LNA miR-25,93,106b/ctrl p=0,001 n=3

Figure 2. **YAP/TAZ transcriptionally regulate *MCM7* and hosted miR-106b-25 cluster**. (**a**) Genomic region around miR-25, 93, 106b cluster in *MCM7* gene. Signal represents normalized read density of YAP, TAZ, TEAD4 and negative control IP (IgG) in ChIP-seq experiments performed in the MDA-MB-231 breast cancer cell line in Zanconato's and collegues's previous work [16]; peaks are regions with significant binding and were obtained as described in the previous work [16]. The coordinates of YAP/TAZ/TEAD4 peaks represented in the figure are the following: chr7:99684587-99685195. (**b,c**) Quantification by real time-PCR of pre-miR-25, 93, 106b and MCM7 transcript level, normalized to GAPDH (left panel) and western blot quantification of MCM7 as measured by densitometry (Uvitec) and normalized to B-actin signal (right panel), in YAP/TAZ interfered H1299 (**b**) and H1975 (**c**) cells. All experiments have been performed at least in triplicate. SEM is indicated. P and n values: H1299 pre-miR-25 siYAP#1TAZ#1/siGFP p=0,0001 n=6, siYAP#2TAZ#2/siGFP p=0,002 n=3, pre-miR-93 siYAP#1TAZ#1/siGFP p=0,007 n=6, siYAP#2TAZ#2/siGFP p=0,004 n=3, pre-miR-106b siYAP#1TAZ#1/siGFP p=0,01 n=6, siYAP#2TAZ#2/siGFP p=0,0009 n=3, MCM7 siYAP#1TAZ#1/siGFP p=0,0004 n=3, siYAP#2TAZ#2/siGFP p=0,01 n=3. H1975 pre-miR-25 siYAP#1TAZ#1/siGFP p=0,004 n=3, siYAP#2TAZ#2/siGFP p=0,009 n=4, pre-miR-93 siYAP#1TAZ#1/siGFP p=0,01 n=3, siYAP#2TAZ#2/siGFP p=0,003 n=3, pre-miR-106b siYAP#1TAZ#1/siGFP p=0,02 n=3, siYAP#2TAZ#2/siGFP p=0,007 n=3, MCM7 siYAP#1TAZ#1/siGFP p=0,004 n=3, siYAP#2TAZ#2/siGFP p=0,003 n=3.

Figure 3. YAP directly binds MCM7 enhancer in NSCLC. TEAD cooperates with YAP and TAZ in the transcriptional regulation of MCM7 and hosted miR-25,93 and 106b.

(**a, b**) TaqMan based PCR quantification of miR-25, 93 and 106b normalized to RNU48 (left panel) and quantification by real time-PCR of pre-miR-25, 93, 106b and MCM7 transcript level, normalized to GAPDH (right panels) in H1299 (**a**) and H1975 (**b**) cells.

H1299 P and n values: pre-miR-25 siYAP#1TEAD1#1/siGFP p=0,001 n=4, pre-miR-93 siTEAD#1/siGFP p=0,01 n=4, siYAP#1TEAD1#1/siGFP p=0,04 n=4, pre-miR-106b siTEAD#1/siGFP p=0,01 n=4, siYAP#1TEAD1#1/siGFP p=0,01 n=4, MCM7 siYAP#1TEAD1#1/siGFP p=0,02 n=4. H1975 p and n values: pre-miR-25 siTEAD#1/siGFP p=0,01 n=3, siYAP#1TEAD1#1/siGFP p=0,006 n=4, pre-miR-93 siTEAD#1/siGFP p=0,02 n=4, siYAP#1TEAD1#1/siGFP p=0,008 n=4, pre-miR-106b siYAP#1TEAD1#1/siGFP p=0,02 n=4, MCM7 siYAP#1TEAD#1/siGFP p=0,01 n=4. (**c, d**) Quantification by real time-PCR of YAP, TEAD1, CTGF and ANKRD1 transcript level, normalized to GAPDH, in H1299 (**c**) and H1975 (**d**) cells. All experiments have been performed at least in triplicate. SEM is indicated. H1299 p and n values: YAP siYAP#1TEAD#1/siGFP p=3,6x10^-5 n=5, TEAD1 siTEAD#1/siGFP p=6,2x10^-6 n=5, siYAP#1TEAD#1/siGFP p=2,6x10^-7 n=5, CTGF siTEAD#1/siGFP p=0,03 n=9, siYAP#1TEAD1#1/siGFP p=8,9x10^6 n=9, ANKRD1 siTEAD1#1/siGFP p=0,01 n=6, siYAP#1TEAD1#1/siGFP p=5,8x10^-7 n=7. H1975 p and n values: YAP siYAP#1TEAD1#1/siGFP p=0,0002 n=4, TEAD1 siTEAD#1/siGFP p=0,003 n=3, siYAP#1TEAD#1/siGFP p=9,5 x10^-6 n=4, CTGF siTEAD#1/siGFP p=0,01 n=3, siYAP#1TEAD1#1/siGFP p=0,001 n=4, ANKRD1 siTEAD#1/siGFP p=0,04 n=4, siYAP#1TEAD1#1/siGFP p=0,01 n=4. (**e, f**) ChIP-qPCR performed on the promoter of YAP direct target *CTGF* [50] and on *MCM7* enhancer found as a YAP/TAZ target in ref. [16]. *CTGF* promoter and *MCM7* enhancer sequences were enriched in YAP-immunoprecipitated chromatin (grey) but not in negative control IP (IgG, black) or in immunoprecipitated chromatin obtained from YAP-depleted cells. Moreover, YAP binding was not detected on negative control (*H1H2BA*, promoter of histone H2B type 1-A). Charts are relative to a representative experiment for each cell line. Two-tailed t test analysis was applied to calculate the p values. H1299 *CTGF* prom: siGFP-αIGG/siGFP-αYAP: p=0,03; siGFP-αYAP/siYAP-αYAP: p=0,004; *MCM7* enhancer: siGFP-αIGG/siGFP-αYAP:

p=0,001; siGFP-αYAP/siYAP-αYAP: p=0,0002. H1975: *CTGF* prom: siGFP-αIGG/siGFP-αYAP: p=0,0001; siGFP-αYAP/siYAP#1-αYAP: p=0,03; *MCM7* enhancer: siGFP-αIGG/siGFP-αYAP: p=0,0006 siGFP-αYAP/siYAP#1-αYAP: p=0,005.

Figure 4. In lung tumour, miR-106b-25 cluster and *MCM7* host gene are overexpressed while p21 is downregulated compared to normal tissue. (**a**) Boxplots representing the relative abundance of mi-R25, 93, 106b and MCM7 transcript in tumoral compared to normal tissue in lung TCGA casuistry. N patients= 470 T, 56 N. (**b**) Pathways predicted to be affected by miR-106b-25 cluster. $-10*\log_{10}$(FDR) was used as a relevance score (see Supplementary table S3). (**c**) Boxplot comparing p21 transcript abundance in tumoral compared to normal tissue in lung TCGA casuistry.

Figure 5. In NSCLC cells, p21 is derepressed upon YAP/TAZ and TEAD1 knock-down. (**a**) Western blot representing YAP, TAZ and p21 protein abundance in H1299 cells, as measured by densitometry (Uvitec) and normalized to B-actin signal after YAP, TAZ, YAP/TAZ interference (left panel) and YAP, TEAD1, YAP/TEAD1 interference (right panel) compared to control counterparts. (**b**) Quantification by real time-PCR of p21 transcript levels, normalized to GAPDH, in siYAP, siTAZ, si YAP/TAZ, siTEAD1 and siYAP/TEAD1 H1299 cells respect to control counterparts. SEM is indicated. Asteriscs represent statistically relevant results. P and n values: p21 siYAP#1/siGFP p=0,005 n=9; siTAZ#1/siGFP p=0,03 n=3; si YAP#1TAZ#1/siGFP p=0,004 n=6; siTEAD1#1/siGFP p=0,03 n=6; siYAP#1TEAD1#1/siGFPp=0,01 n=5. **(c, d)** As described in Figures (**a, b**) but for the H1975 cell line. SEM is indicated. P and n values: p21 siYAP#1/siGFP p=0,01 n=7; siTAZ#1/siGFP p=0,002 n=6; siYAP#1TAZ#1/siGFP p=0,006 n=5; siTEAD1#1/siGFP p=0,02 n=4; siYAP#1TEAD1#1/siGFP p=0,01 n=4. (**e**) Schematic representation of different mechanisms through which YAP/TAZ may regulate p21 protein abundance as

shown in previous works (left and right panels, [37] [38]) and as shown in our study (mid panel).

Figure 6. **YAP/TAZ elicit their oncogenic function by simultaneously regulating *MCM7* gene and hosted miR-25, 93, 106b cluster that in turn inhibit p21 and affect cell proliferation.** (**a**) Western blot showing MCM7 and p21 protein abundance, normalized to B-actin, in cells knocked down for MCM7 with two alternative siRNAs (siMCM7#1 and siMCM7#2) compared to control siGFP H1299 cells. (**b**) Quantification by real time-PCR of p21 transcript levels, normalized to GAPDH, in cells knocked down for MCM7 compared to siGFP control cells. P and n values: H1299 p21 siMCM7#2 p=0,04 n=4. (**c,d**) Same as (**a,b**) but for H1975 cell line. P and n values: H1975 p21 siMCM7#1 p=0,006 n=3; siMCM7#2 p=0,03 n=3. (**e,f**) Western blot showing MCM7 and p21 protein abundance as measured by densitometry and normalized to B-actin (left panel), and real-time quantification of their transcripts normalized to GAPDH (right panel) in H1299 cells treated with LNA inhibitors for miR-25, 93 and 106b (**e**) and H1975 cell line (**f**). All the experiments were performed in triplicate. (**g**) Cartoon representing the newly characterized mechanism through which YAP/TAZ and TEAD by binding to *MCM7* enhancer transcriptionally regulate both *MCM7* gene and the hosted miR cluster miR-25, 93 and 106b, that in turn post-transcriptionally regulate p21 abundance eventually affecting cell proliferation (left panel). Treatment of cells with statin determines YAP/TAZ exclusion from nuclei, impairs transcription of *MCM7* gene and hosted miRs cluster and derepresses p21 thus inhibiting cell proliferation (right panel).

Funding

This work was supported by the Italian Association for Cancer Research (AIRC) (Grant n.14455) and from Epigenomics Flagship Project (EPIGEN; sub- project 7.6) to G.B, AIRC

triennial fellowship "Starwood Hotels & Resorts" to L.S.F. and by the Italian Ministry of Health RF-2011-02346976 and the Italian Association for Cancer Research (AIRC) to Special Program Molecular Clinical Oncology “5 per mille” (Grant n. 10016), and AIRC IG-grant 17659 to GDS.

Aknowlegments

We thank Dr. Arnold Gruenweller, Philipps-Marburg University, 35032 Marburg, for kindly providing p21-3’UTR-firefly luciferase reporter and pGL3 empty vector. We thank Federica Ganci and Francesca Biagioni for sharing their published datasets on breast cancer and Head and Neck cancer casuistry.

Author contribution: F.L.S designed and performed all the experiments. A.S and M.F conducted all *bioinformatics analyses. V.C performed experiments with cerivastatin. F.Z,* S.D.A, S.S, S.B, G.D.S contributed to the critical reading of the manuscript and suggested some experiments, G.B acquired funding, planned experiments and *bioinformatics analyses* and contributed to the critical reading of the manuscript.

Conflict of Interest Statement: None declared.

References

1. Jemal A, Siegel R, Ward E, Hao Y, Xu J, Thun MJ. Cancer statistics, 2009. CA Cancer J Clin. 2009;59(4):225-49. doi: 10.3322/caac.20006. PubMed PMID: 19474385.
2. Siegel R, Naishadham D, Jemal A. Cancer statistics, 2013. CA Cancer J Clin. 2013;63(1):11-30. doi: 10.3322/caac.21166. PubMed PMID: 23335087.
3. Ferlay J, Shin HR, Bray F, Forman D, Mathers C, Parkin DM. Estimates of worldwide burden of cancer in 2008: GLOBOCAN 2008. Int J Cancer. 2010;127(12):2893-917. doi: 10.1002/ijc.25516. PubMed PMID: 21351269.
4. Hansen CG, Moroishi T, Guan KL. YAP and TAZ: a nexus for Hippo signaling and beyond. Trends Cell Biol. 2015;25(9):499-513. doi: 10.1016/j.tcb.2015.05.002. PubMed PMID: 26045258; PubMed Central PMCID: PMC4554827.
5. Moroishi T, Hansen CG, Guan KL. The emerging roles of YAP and TAZ in cancer. Nat Rev Cancer. 2015;15(2):73-9. doi: 10.1038/nrc3876. PubMed PMID: 25592648.
6. Su LL, Ma WX, Yuan JF, Shao Y, Xiao W, Jiang SJ. Expression of Yes-associated protein in non-small cell lung cancer and its relationship with clinical pathological factors. Chin Med J (Engl). 2012;125(22):4003-8. Epub 2012/11/20. PubMed PMID: 23158133.
7. Wang Y, Dong Q, Zhang Q, Li Z, Wang E, Qiu X. Overexpression of yes-associated protein contributes to progression and poor prognosis of non-small-cell lung cancer. Cancer Sci. 2010;101(5):1279-85. doi: 10.1111/j.1349-7006.2010.01511.x. PubMed PMID: 20219076.
8. Zhou Z, Hao Y, Liu N, Raptis L, Tsao MS, Yang X. TAZ is a novel oncogene in non-small cell lung cancer. Oncogene. 2011;30(18):2181-6. doi: 10.1038/onc.2010.606. PubMed PMID: 21258416.
9. Hsu YL, Hung JY, Chou SH, Huang MS, Tsai MJ, Lin YS, et al. Angiomotin decreases lung cancer progression by sequestering oncogenic YAP/TAZ and decreasing Cyr61 expression. Oncogene. 2014. doi: 10.1038/onc.2014.333. PubMed PMID: 25381822.
10. Strazisar M, Mlakar V, Glavac D. LATS2 tumour specific mutations and down-regulation of the gene in non-small cell carcinoma. Lung Cancer. 2009;64(3):257-62. doi: 10.1016/j.lungcan.2008.09.011. PubMed PMID: 19008013.
11. Lau AN, Curtis SJ, Fillmore CM, Rowbotham SP, Mohseni M, Wagner DE, et al. Tumor-propagating cells and Yap/Taz activity contribute to lung tumor progression and metastasis. EMBO J. 2014;33(5):468-81. doi: 10.1002/embj.201386082. PubMed PMID: 24497554; PubMed Central PMCID: PMC3989628.
12. Beyer TA, Weiss A, Khomchuk Y, Huang K, Ogunjimi AA, Varelas X, et al. Switch Enhancers Interpret TGF-beta and Hippo Signaling to Control Cell Fate in Human Embryonic Stem Cells. Cell Rep. 2013;5(6):1611-24. Epub 2013/12/18. doi: S2211-1247(13)00688-8 [pii]

10.1016/j.celrep.2013.11.021. PubMed PMID: 24332857.
13. Zhao B, Ye X, Yu J, Li L, Li W, Li S, et al. TEAD mediates YAP-dependent gene induction and growth control. Genes Dev. 2008;22(14):1962-71. doi: 10.1101/gad.1664408. PubMed PMID: 18579750; PubMed Central PMCID: PMC2492741.
14. Mizuno T, Murakami H, Fujii M, Ishiguro F, Tanaka I, Kondo Y, et al. YAP induces malignant mesothelioma cell proliferation by upregulating transcription of cell cycle-promoting genes. Oncogene. 2012;31(49):5117-22. doi: 10.1038/onc.2012.5. PubMed PMID: 22286761.
15. Lian I, Kim J, Okazawa H, Zhao J, Zhao B, Yu J, et al. The role of YAP transcription coactivator in regulating stem cell self-renewal and differentiation. Genes Dev.

2010;24(11):1106-18. doi: 10.1101/gad.1903310. PubMed PMID: 20516196; PubMed Central PMCID: PMC2878649.
16. Zanconato F, Forcato M, Battilana G, Azzolin L, Quaranta E, Bodega B, et al. Genome-wide association between YAP/TAZ/TEAD and AP-1 at enhancers drives oncogenic growth. Nat Cell Biol. 2015;17(9):1218-27. doi: 10.1038/ncb3216. PubMed PMID: 26258633.
17. Shen Z, Stanger BZ. YAP regulates S-phase entry in endothelial cells. PLoS One. 2015;10(1):e0117522. doi: 10.1371/journal.pone.0117522. PubMed PMID: 25635998; PubMed Central PMCID: PMC4312014.
18. Stein C, Bardet AF, Roma G, Bergling S, Clay I, Ruchti A, et al. YAP1 Exerts Its Transcriptional Control via TEAD-Mediated Activation of Enhancers. PLoS Genet. 2015;11(8):e1005465. doi: 10.1371/journal.pgen.1005465. PubMed PMID: 26295846; PubMed Central PMCID: PMC4546604.
19. Tumaneng K, Schlegelmilch K, Russell RC, Yimlamai D, Basnet H, Mahadevan N, et al. YAP mediates crosstalk between the Hippo and PI(3)K-TOR pathways by suppressing PTEN via miR-29. Nat Cell Biol. 2012;14(12):1322-9. doi: 10.1038/ncb2615. PubMed PMID: 23143395; PubMed Central PMCID: PMC4019071.
20. Bertero T, Cottrill KA, Lu Y, Haeger CM, Dieffenbach P, Annis S, et al. Matrix Remodeling Promotes Pulmonary Hypertension through Feedback Mechanoactivation of the YAP/TAZ-miR-130/301 Circuit. Cell Rep. 2015;13(5):1016-32. doi: 10.1016/j.celrep.2015.09.049. PubMed PMID: 26565914; PubMed Central PMCID: PMC4644508.
21. Poliseno L, Salmena L, Riccardi L, Fornari A, Song MS, Hobbs RM, et al. Identification of the miR-106b~25 microRNA cluster as a proto-oncogenic PTEN-targeting intron that cooperates with its host gene MCM7 in transformation. Sci Signal. 2010;3(117):ra29. Epub 2010/04/15. doi: 3/117/ra29 [pii]

10.1126/scisignal.2000594. PubMed Central PMCID: PMCPMC2982149.
22. Ganci F, Sacconi A, Bossel Ben-Moshe N, Manciocco V, Sperduti I, Strigari L, et al. Expression of TP53 mutation-associated microRNAs predicts clinical outcome in head and neck squamous cell carcinoma patients. Ann Oncol. 2013;24(12):3082-8. doi: 10.1093/annonc/mdt380. PubMed PMID: 24107801; PubMed Central PMCID: PMC3841017.
23. Ivanovska I, Ball AS, Diaz RL, Magnus JF, Kibukawa M, Schelter JM, et al. MicroRNAs in the miR-106b family regulate p21/CDKN1A and promote cell cycle progression. Mol Cell Biol. 2008;28(7):2167-74. Epub 2008/01/24. doi: MCB.01977-07 [pii]

10.1128/MCB.01977-07. PubMed Central PMCID: PMCPMC2268421.
24. Yoshida K, Inoue I. Conditional expression of MCM7 increases tumor growth without altering DNA replication activity. FEBS Lett. 2003;553(1-2):213-7. PubMed PMID: 14550576.
25. Ren B, Yu G, Tseng GC, Cieply K, Gavel T, Nelson J, et al. MCM7 amplification and overexpression are associated with prostate cancer progression. Oncogene. 2006;25(7):1090-8. doi: 10.1038/sj.onc.1209134. PubMed PMID: 16247466.
26. Erkan EP, Strobel T, Lewandrowski G, Tannous B, Madlener S, Czech T, et al. Depletion of minichromosome maintenance protein 7 inhibits glioblastoma multiforme tumor growth in vivo. Oncogene. 2014;33(39):4778-85. doi: 10.1038/onc.2013.423. PubMed PMID: 24166506.
27. Fujioka S, Shomori K, Nishihara K, Yamaga K, Nosaka K, Araki K, et al. Expression of minichromosome maintenance 7 (MCM7) in small lung adenocarcinomas (pT1): Prognostic implication. Lung Cancer. 2009;65(2):223-9. doi: 10.1016/j.lungcan.2008.11.007. PubMed PMID: 19144445.
28. Toyokawa G, Masuda K, Daigo Y, Cho HS, Yoshimatsu M, Takawa M, et al. Minichromosome Maintenance Protein 7 is a potential therapeutic target in human cancer and a novel prognostic marker of non-small cell lung cancer. Mol Cancer. 2011;10:65. doi: 10.1186/1476-4598-10-65. PubMed PMID: 21619671; PubMed Central PMCID: PMC3125391.

29. Liu YZ, Jiang YY, Hao JJ, Lu SS, Zhang TT, Shang L, et al. Prognostic significance of MCM7 expression in the bronchial brushings of patients with non-small cell lung cancer (NSCLC). Lung Cancer. 2012;77(1):176-82. doi: 10.1016/j.lungcan.2012.03.001. PubMed PMID: 22456526.
30. Forsburg SL. The MCM helicase: linking checkpoints to the replication fork. Biochem Soc Trans. 2008;36(Pt 1):114-9. doi: 10.1042/BST0360114. PubMed PMID: 18208397.
31. Zhang H, Liu CY, Zha ZY, Zhao B, Yao J, Zhao S, et al. TEAD transcription factors mediate the function of TAZ in cell growth and epithelial-mesenchymal transition. J Biol Chem. 2009;284(20):13355-62. Epub 2009/03/28. doi: M900843200 [pii]

10.1074/jbc.M900843200. PubMed PMID: 19324877; PubMed Central PMCID: PMC2679435.
32. Hiemer SE, Szymaniak AD, Varelas X. The Transcriptional Regulators TAZ and YAP Direct Transforming Growth Factor beta-induced Tumorigenic Phenotypes in Breast Cancer Cells. J Biol Chem. 2014;289(19):13461-74. Epub 2014/03/22. doi: M113.529115 [pii]

10.1074/jbc.M113.529115.
33. Sorrentino G, Ruggeri N, Specchia V, Cordenonsi M, Mano M, Dupont S, et al. Metabolic control of YAP and TAZ by the mevalonate pathway. Nat Cell Biol. 2014;16(4):357-66. Epub 2014/03/25. doi: ncb2936 [pii]

10.1038/ncb2936. PubMed PMID: 24658687.
34. Di Agostino S, Sorrentino G, Ingallina E, Valenti F, Ferraiuolo M, Bicciato S, et al. YAP enhances the pro-proliferative transcriptional activity of mutant p53 proteins. EMBO Rep. 2016;17(2):188-201. doi: 10.15252/embr.201540488. PubMed PMID: 26691213.
35. Taccioli C, Sorrentino G, Zannini A, Caroli J, Beneventano D, Anderlucci L, et al. MDP, a database linking drug response data to genomic information, identifies dasatinib and statins as a combinatorial strategy to inhibit YAP/TAZ in cancer cells. Oncotarget. 2015;6(36):38854-65. doi: 10.18632/oncotarget.5749. PubMed PMID: 26513174; PubMed Central PMCID: PMC4770742.
36. Biagioni F, Bossel Ben-Moshe N, Fontemaggi G, Canu V, Mori F, Antoniani B, et al. miR-10b*, a master inhibitor of the cell cycle, is down-regulated in human breast tumours. EMBO Mol Med. 2012;4(11):1214-29. doi: 10.1002/emmm.201201483. PubMed PMID: 23125021; PubMed Central PMCID: PMC3494877.
37. Vitolo MI, Anglin IE, Mahoney WM, Jr., Renoud KJ, Gartenhaus RB, Bachman KE, et al. The RUNX2 transcription factor cooperates with the YES-associated protein, YAP65, to promote cell transformation. Cancer Biol Ther. 2007;6(6):856-63. PubMed PMID: 17438369.
38. Muramatsu T, Imoto I, Matsui T, Kozaki K, Haruki S, Sudol M, et al. YAP is a candidate oncogene for esophageal squamous cell carcinoma. Carcinogenesis. 2011;32(3):389-98. Epub 2010/11/30. doi: bgq254 [pii]

10.1093/carcin/bgq254. PubMed PMID: 21112960.
39. Chaulk SG, Lattanzi VJ, Hiemer SE, Fahlman RP, Varelas X. The Hippo pathway effectors TAZ/YAP regulate dicer expression and microRNA biogenesis through Let-7. J Biol Chem. 2014;289(4):1886-91. doi: 10.1074/jbc.C113.529362. PubMed PMID: 24324261; PubMed Central PMCID: PMC3900939.
40. Mori M, Triboulet R, Mohseni M, Schlegelmilch K, Shrestha K, Camargo FD, et al. Hippo signaling regulates microprocessor and links cell-density-dependent miRNA biogenesis to cancer. Cell. 2014;156(5):893-906. doi: 10.1016/j.cell.2013.12.043. PubMed PMID: 24581491; PubMed Central PMCID: PMC3982296.
41. Louie MC, Revenko AS, Zou JX, Yao J, Chen HW. Direct control of cell cycle gene expression by proto-oncogene product ACTR, and its autoregulation underlies its

transforming activity. Mol Cell Biol. 2006;26(10):3810-23. doi: 10.1128/MCB.26.10.3810-3823.2006. PubMed PMID: 16648476; PubMed Central PMCID: PMC1489001.
42. Wei Q, Li J, Liu T, Tong X, Ye X. Phosphorylation of minichromosome maintenance protein 7 (MCM7) by cyclin/cyclin-dependent kinase affects its function in cell cycle regulation. J Biol Chem. 2013;288(27):19715-25. doi: 10.1074/jbc.M112.449652. PubMed PMID: 23720738; PubMed Central PMCID: PMC3707676.
43. Poliseno L, Pandolfi PP. PTEN ceRNA networks in human cancer. Methods. 2015;77-78:41-50. doi: 10.1016/j.ymeth.2015.01.013. PubMed PMID: 25644446.
44. Ferrarelli LK. Focus issue: noncoding RNAs in cancer. Sci Signal. 2015;8(368):eg3. doi: 10.1126/scisignal.aaa9789. PubMed PMID: 25783156.
45. Kron KJ, Bailey SD, Lupien M. Enhancer alterations in cancer: a source for a cell identity crisis. Genome Med. 2014;6(9):77. doi: 10.1186/s13073-014-0077-3. PubMed PMID: 25473436; PubMed Central PMCID: PMC4254433.
46. Leveille N, Melo CA, Agami R. Enhancer-associated RNAs as therapeutic targets. Expert Opin Biol Ther. 2015;15(5):723-34. doi: 10.1517/14712598.2015.1029452. PubMed PMID: 25819025.
47. Freed-Pastor WA, Mizuno H, Zhao X, Langerod A, Moon SH, Rodriguez-Barrueco R, et al. Mutant p53 disrupts mammary tissue architecture via the mevalonate pathway. Cell. 2012;148(1-2):244-58. doi: 10.1016/j.cell.2011.12.017. PubMed PMID: 22265415; PubMed Central PMCID: PMC3511889.
48. Nielsen SF, Nordestgaard BG, Bojesen SE. Statin use and reduced cancer-related mortality. N Engl J Med. 2013;368(6):576-7. doi: 10.1056/NEJMc1214827. PubMed PMID: 23388012.
49. Huang da W, Sherman BT, Lempicki RA. Bioinformatics enrichment tools: paths toward the comprehensive functional analysis of large gene lists. Nucleic Acids Res. 2009;37(1):1-13. doi: 10.1093/nar/gkn923. PubMed PMID: 19033363; PubMed Central PMCID: PMC2615629.
50. Huang da W, Sherman BT, Lempicki RA. Systematic and integrative analysis of large gene lists using DAVID bioinformatics resources. Nat Protoc. 2009;4(1):44-57. doi: 10.1038/nprot.2008.211. PubMed PMID: 19131956.

Figure 1

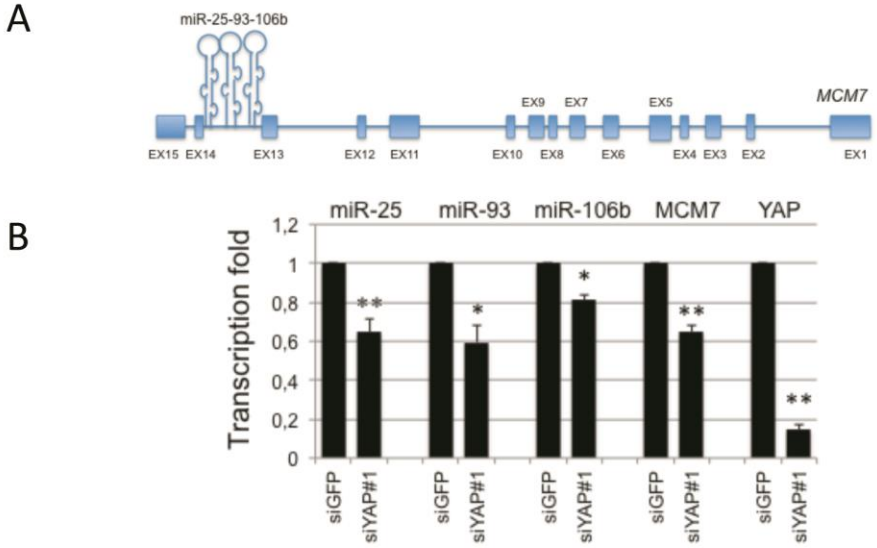

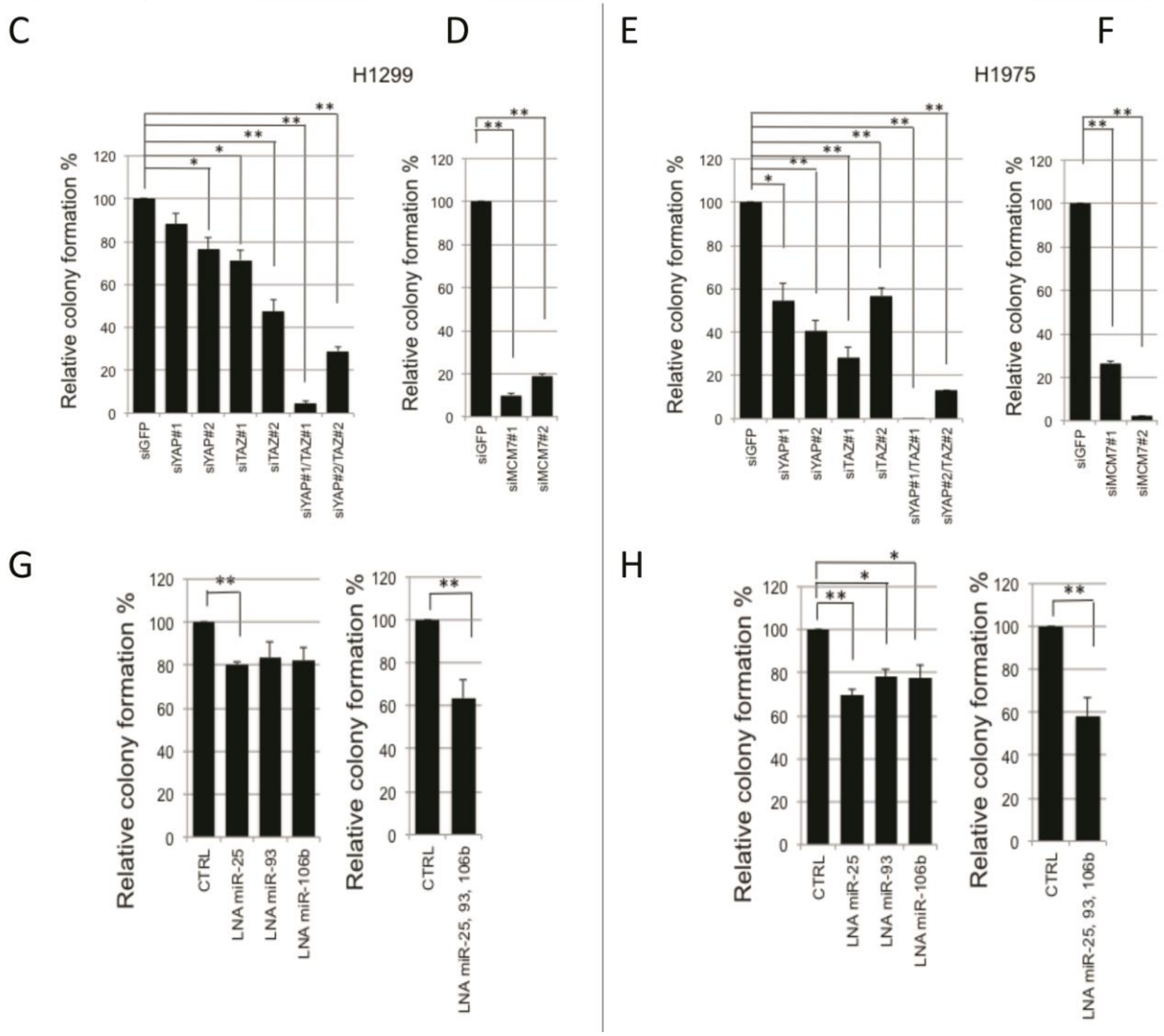

Figure 2

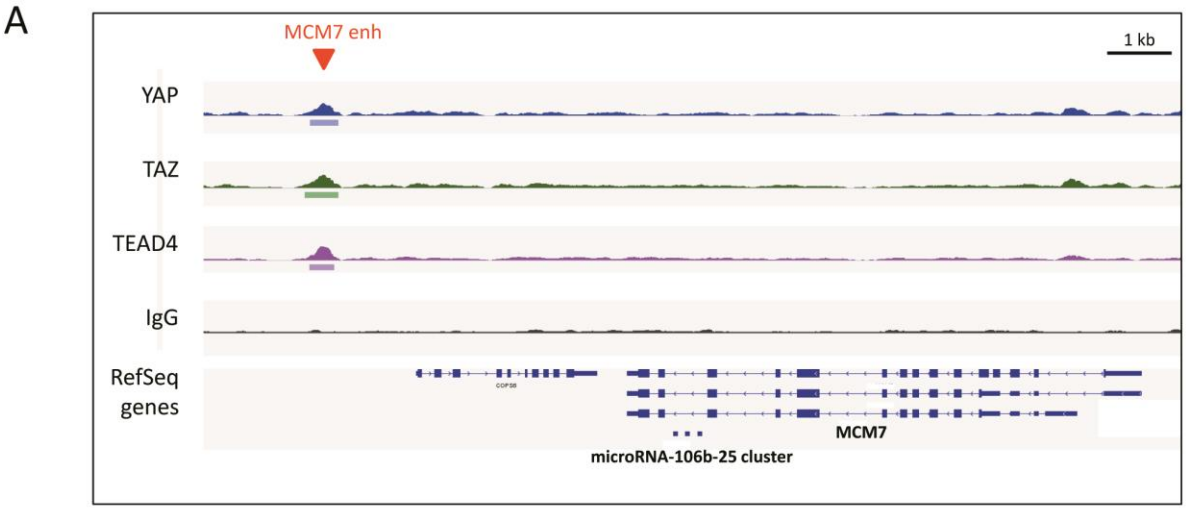

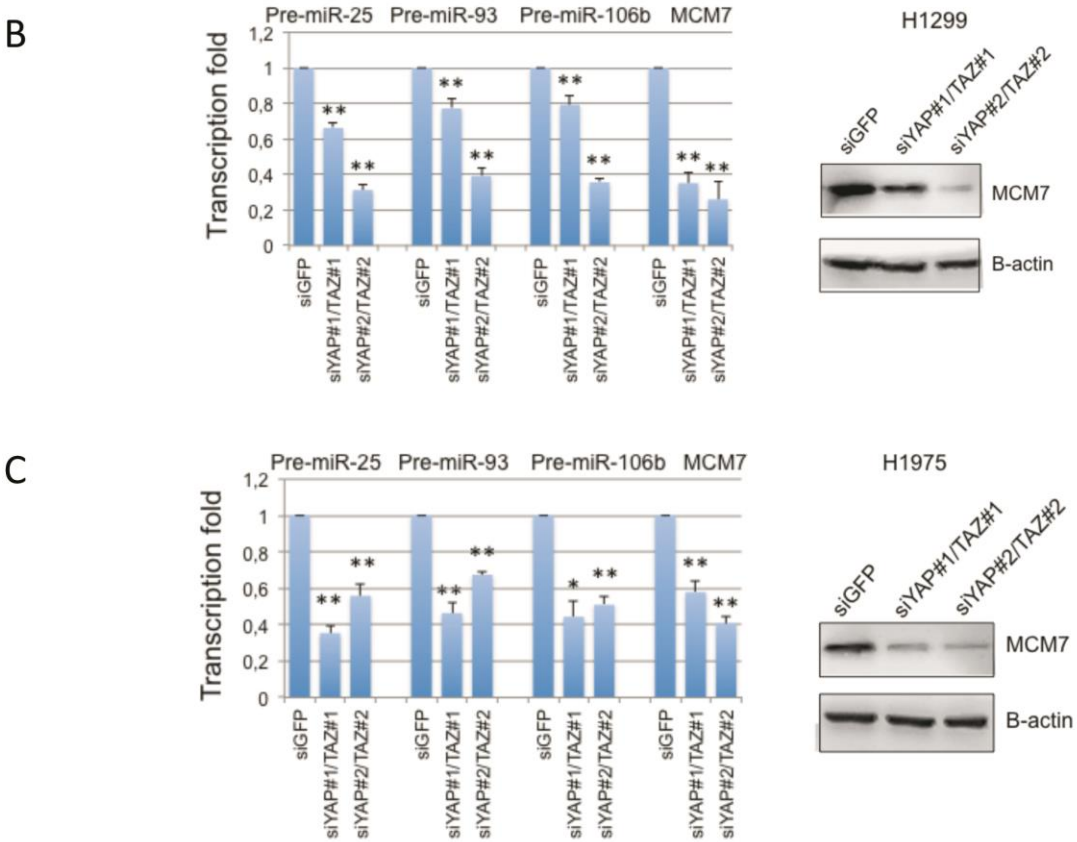

Figure 3

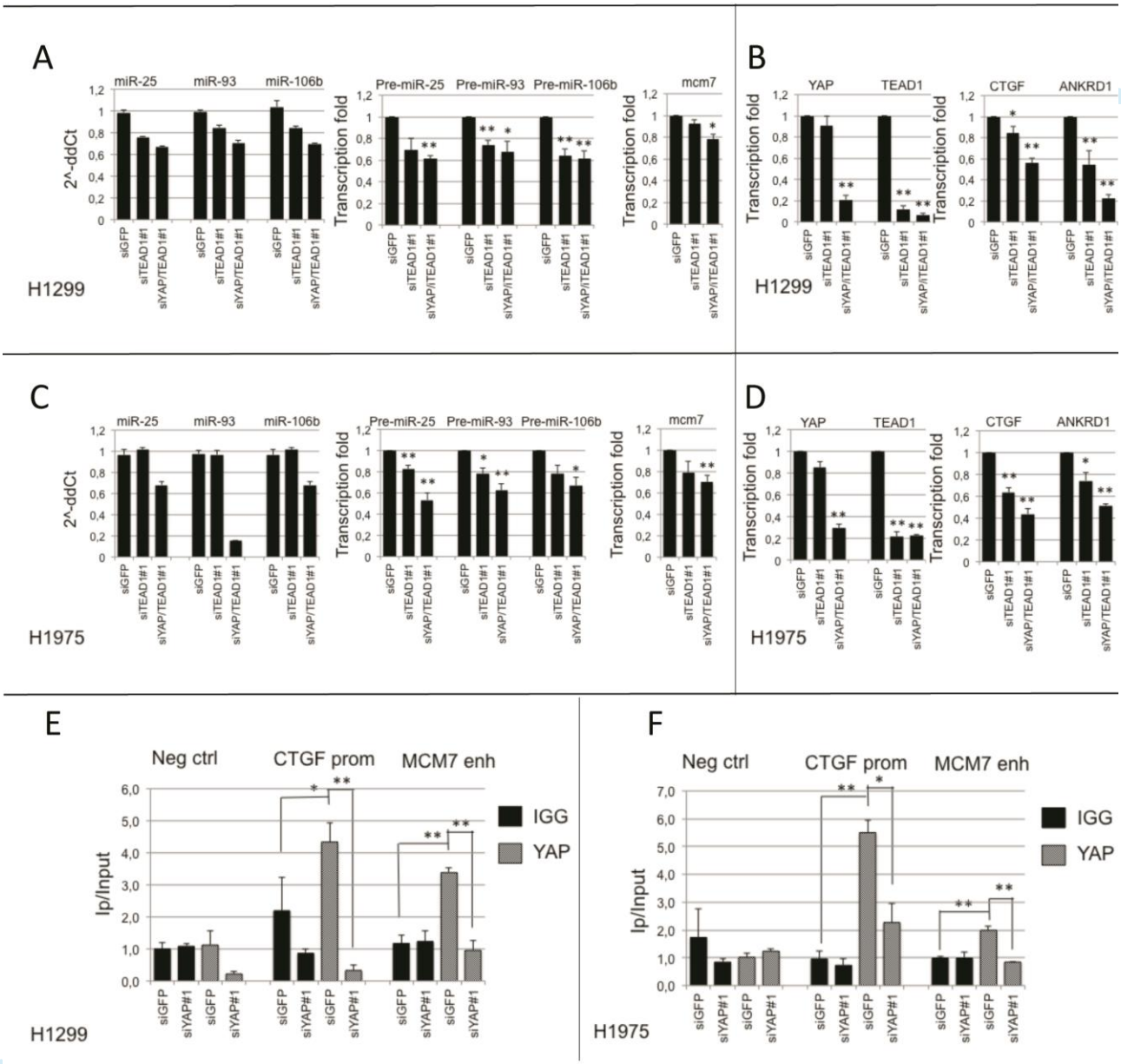

Figure 4

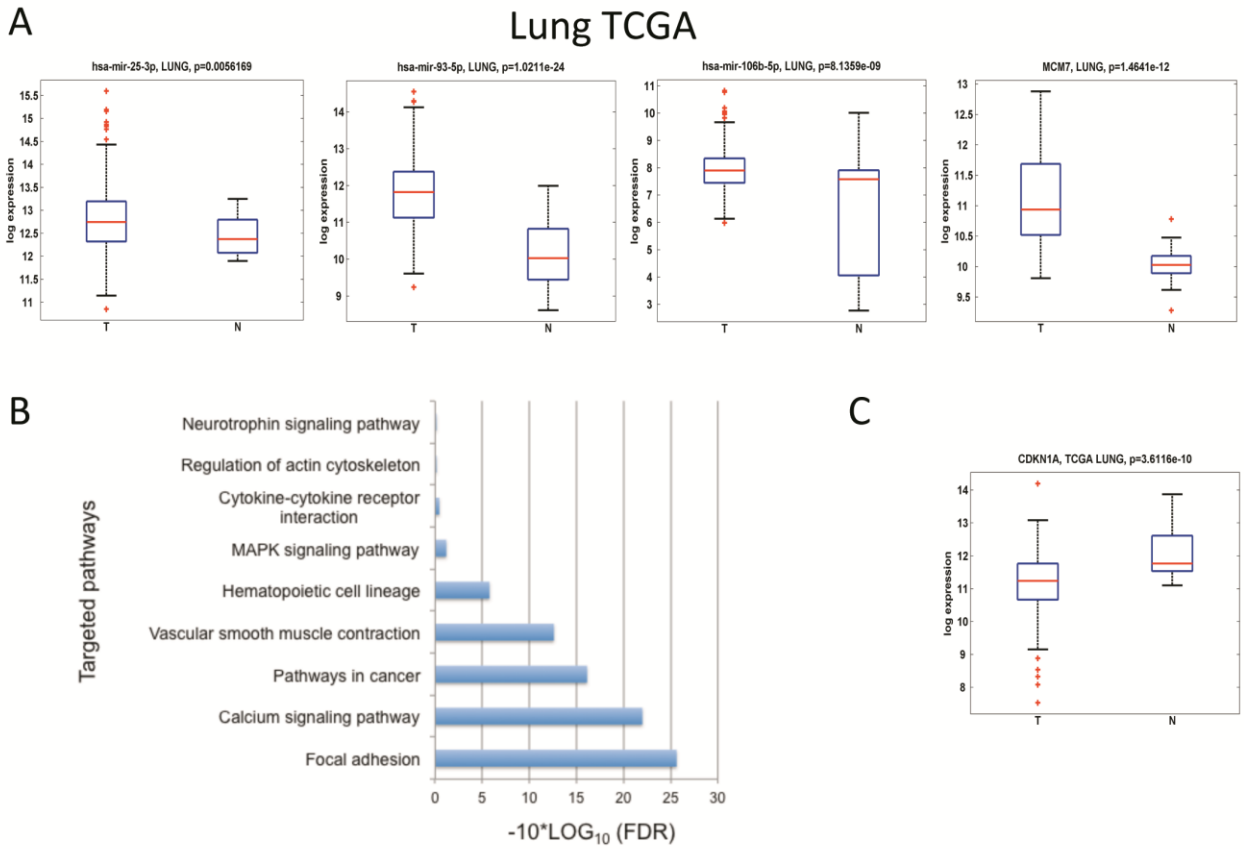

Figure 5

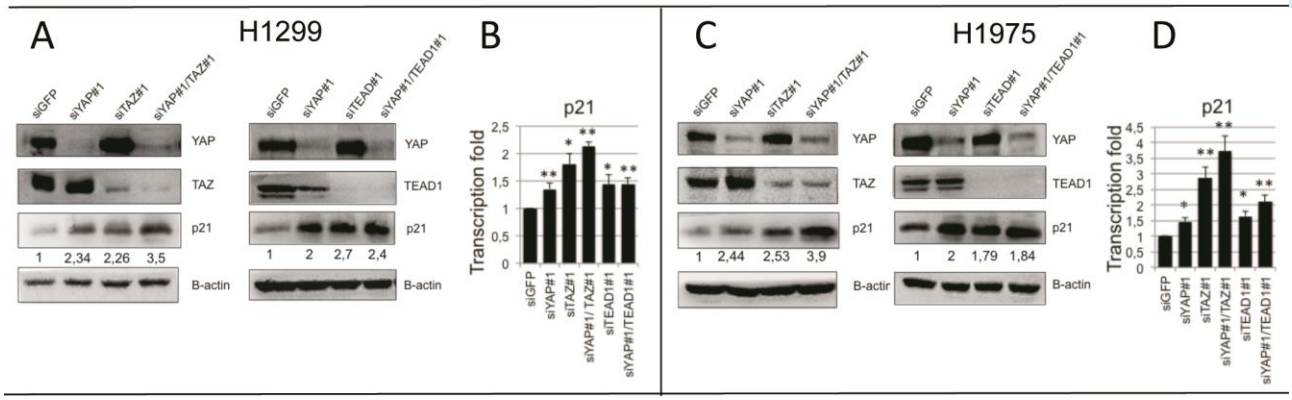

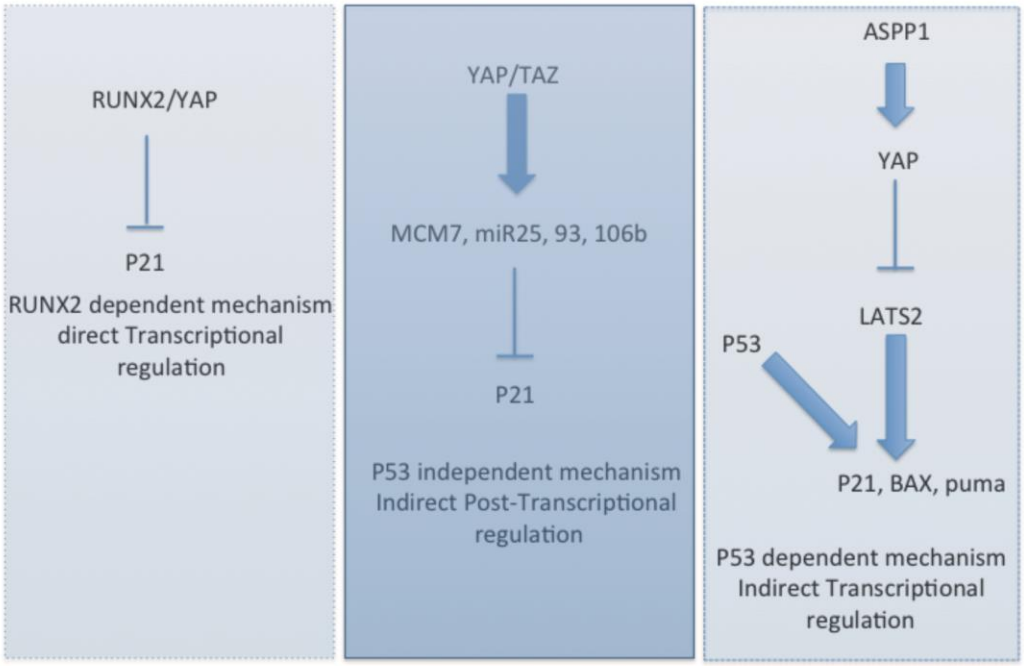

Figure 6